Manipulating Connectivity to Control Fracture in Network Polymer Adhesives

Mark J. Stevens

P.O. Box 5800, MS 1111, Sandia National Laboratories, Albuquerque, New Mexico 87185-1111

Received May 31, 2000; Revised Manuscript Received November 17, 2000

ABSTRACT: Coarse-grained molecular dynamics (MD) simulations are applied to fracture in highly cross-linked, polymer networks. Random polymer networks between two solid surfaces are created by simulating the dynamical cross-linking process. Simple, ordered networks are constructed geometrically, which enables easy manipulation of the network connectivity. The failure strain of tensile pull and shear simulations is related to the minimal paths through the network connecting the solid surfaces. This result is confirmed by using the ordered networks to explicity vary the minimal paths over a very wide range. Failure strains are constructed in the ordered systems to be either larger or smaller than the dynamically formed networks. The constraints imposed by the network connectivity control the tightness of local deformations.

I. Introduction

Progress in atomic aspects of fracture has recently occurred through simulations for bulk crystals.[1,2] Less work exists for amorphous materials like polymers.[3] Since the typical adhesive material is a polymer network, the interfacial fracture of polymer adhesives bonded to a solid surface is a fundamental and practical problem.[4] Highly cross-linked polymer networks have been particularly neglected by simulations, yet they are an important class of adhesives. While linear elastic fracture mechanics works well for such polymers far from the crack tip, the method breaks down near the crack tip where large plastic deformation occurs and the molecular details become important.[4] Experimentally, it is known that as the cross-link density increases, the failure mechanism changes from crazes to deformation zones.[5] This article reports molecular dynamics simulations of highly cross-linked polymer networks bonded to a solid surface focusing on aspects of the role of connectivity.

In a random network, the stress on bonds is expected to vary, and the network bonds that are most stressed will break first.[6] The spatial distribution of bond breaking events is expected to be random at least initially. Crack initiation should occur where a cluster of highly constrained bonds exists.

Molecular dynamics (MD) simulations can treat the complexities of interfacial polymer fracture. Simple coarse-grained bead−spring models have been successful in treating bulk polymer networks and melts to interfacial fracture.[7,8] Recently, these methods have been used to treat fracture in highly cross-linked polymers.[9] Connectivity is an essential ingredient in polymer dynamics[10] and in simulations of fiber fracture.[11] The bead−spring models preserve the connectivity with more molecular detail than in simple lattice models.[11]

Using coarse-grained MD, highly cross-linked networks are formed between and bonded to solid surfaces. The molecular deformation sequence is determined for an applied tensile strain. The failure strain is shown to be related to the minimal paths through the network between the two solid surfaces. The network connectivity is a critical determinant of many aspects of the fracture. To demonstrate the effect of differing connectivities a very simple model is developed. This model system is more amenable to manipulation and theoretical treatment. Using this model, the minimal paths are explicity varied and the failure strain is demonstrated to be determined by the minimal paths.

II. Simulation Method

Polymer chains are composed of beads interacting via a Lennard-Jones (LJ) potential with a cutoff at 2.5.[8] All quantities will be in LJ units; σ and ϵ represent the stress and the strain. Typically in these models, beads would be bonded together by a finite-extensible nonlinear elastic (FENE) bond potential preventing chain crossing,[8] but FENE bonds cannot break. To break bonds and preserve the continuity of the bond force, a breakable quartic bond potential was created that approximates the FENE potential at the potential minimum

$$U_4(r) = \begin{cases} k_4(y - b_1)(y - b_2)y^2 + U_0 + U_{\mathrm{RLJ}}(r), & r < r_c \\ U_0 & r \geq r_c \end{cases} \quad (1)$$

where $y = r - \Delta r$ shifts the quartic center from the origin. The potential $U_{\mathrm{RLJ}}(r)$ is the purely repulsive LJ potential which is cutoff at its minimum ($2^{1/6}$) and shifted to be zero at the cutoff. The potential is smoothly cutoff at r_c chosen to be about the typical maximum extent for the FENE potential. Once a bond separation is larger than r_c, the bond is broken and the bond potential between the pair turned off, preventing the bond from reforming. The parameters were determined by fitting the total bond force with the quartic component to the bond force with the FENE component at the first zero and the minimum. This just leaves the maximum bond force as a free variable. The potential parameters used here are as follows: $k_4 = 1200$, $b_1 = -0.55$, $b_2 = 0.25$, $\Delta r = 1.3$, $r_c = 1.47$, and $U_0 = 34.69$. With this bond potential, chains can cross only by breaking bonds.

The maximum bond force is 70, and the maximum LJ force is 2.4. For atomic force fields, the force ratio

10.1021/ma0009505 CCC: $20.00
Published on Web 01/26/2001

between the bond and the van der Waals forces is about 1000 compared to 30 for the simulation parameters. However, a single bead represents several atoms and the LJ pair interaction represents multiple van der Waals pair interactions. With even just three atoms per bead, there are nine pair interactions. A force ratio of order 100 in the coarse-grained model is representative of the atomic system. The ratio 30 in the present simulations is small, but by a factor of less than 10.

The complete system consists of a polymer network between two solid walls. Each wall is two layers of particles in an fcc lattice with nearest neighbor distance 1.204. The (111) direction (z direction) is perpendicular to the walls. The wall particles are bound to the lattice sites by a harmonic spring with spring constant 100. The wall dimensions give the simulation cell lateral lengths, L_x and L_y, and periodic boundary conditions are applied in these directions. The periodic boundary conditions imply that the simulations treat a region in the middle (i.e., far from the edges) of a system with large lateral extent. The separation distance between the innermost wall layers is L_z. The wall particles interact with the beads via the LJ potential,[12] with some wall particles bonded to the polymer network by eq 1. The dynamics is performed at constant temperature T using the Langevin thermostat.[13] The integration time step is 0.005, and the damping constants are 1 for the monomers and 5 for the walls.

To form the networks, we take a cue from an highly cross-linked adhesive, epoxies. Epoxies are chemically cured networks formed from a liquid mixture of a resin (Bisphenol A) and a cross-linker.[14] Each strand consists of only a few monomers. As a bead corresponds typically to two or three monomers,[8] an epoxy model would have only a few beads per strand. The minimal case of two beads is used here. Longer strands will make the network more elastomeric with a larger failure strain. The emphasis is on understanding general features, not on optimally modeling epoxies.

The networks are dynamically formed in a manner similar to epoxy network formation. In epoxies, a liquid mixture of a cross-linker and a resin is cross-linked dynamically. In the simulations the mixture consists of two bead and three bead molecules. The three bead molecule has a 6-fold functional cross-linker bead already bonded to a two bead strand. The strand beads and cross-linker beads have identical potential parameters. Bonds are formed in a simulation when the separation between a cross-linker and a strand end or wall particle is less than 1.3. At each MD time step, the closest end bead to a cross-linker that satisfies the above distance criterion is bonded by turning on the bond potential. Once the cross-linker is fully bonded, no more bonds to it are allowed.

The liquid mixture is equilibrated between the two solid surfaces at $T = 1.2$. Curing then occurs in a two-stage process. First, the liquid is allowed to bond to the solid surface. This process has been been performed in two ways. To promote interfacial failure, only one bond per cross-linker to a wall is allowed. The second way allows the cross-linker to bond as much as it can which typically results in three bonds to the surface per cross-linker. This surface bonding occurs in 100 time steps to allow for particles to move within their local neighborhood. In the second stage, during a MD run cross-linkers are bonded to strands until at least 95% of all possible bonds are made. Zero load is maintained on the walls during the cross-linking allowing the wall separation to contract. Afterward, the temperature is reduced below the glass transition temperature ($T_g = 0.5$) to 0.3. The value of T_g was calculated from bulk constant pressure simulations of the random network using the diffusion constant and the density to determine T_g. Results will be presented for system R1 which has only one bond per cross-linker to the surface. System R1 is a random network with 9800 monomers and initial dimensions $L_x = 19.3$, $L_y = 33.1$, and $L_z = 15.1$. System size effects in random networks are fully discussed in ref 9 and summarized in section IV.

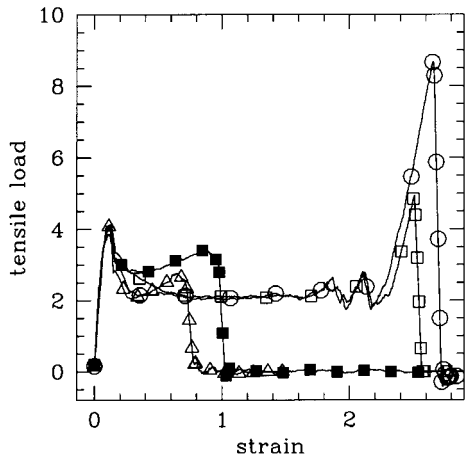

Figure 1. Stress−strain curves for the random network R1 (solid squares) and the ordered networks O1 (squares), O2 (triangles), and O3 (circles).

III. Results

Simulations under both tensile pull and shear conditions have been performed. The discussion will concentrate on the tensile pull simulations with a few comments on the shear simulations. Both deformation modes are achieved by moving the walls at constant velocity in the appropriate directions. In Figure 1, the stress−strain curve is shown for both walls pulled at a wall velocity of 0.01. The yield stress is about $\sigma_y = 4$, and the yield strain is 0.1. The stress drops suddenly, and complete failure occurs at $\epsilon_f = 1.0$ and $\sigma_f = 3.4$. Here, ϵ_f is taken to be the strain at the midpoint of the sharp drop in stress where the stress is $\sigma_f/2$. The first bond breaks at $\epsilon = 0.63$. Between $\epsilon = 0.82$ and 1.0, all the bonds between the network and the bottom wall break, resulting in failure.

For system R1, the vast majority of broken bonds occur at the interface. Bonds in the bulk of the random network are with only a few exceptions not stressed. In fact, strains large compared to macroscopic measurements are required before even the interfacial bonds stretch and finally break. To understand what determines the failure strains and why apparently large strains are required, the molecular deformation sequence was determined by examining configuration images. At low strains, the near neighbor cage is plastically deformed producing the yield behavior. This deformation involves only LJ interactions and determines σ_y. Once the monomers have moved beyond their initial local position, further applied strains tighten the strands of the network. In the plateau region, bond lengths are rarely stretched. The bonds begin to stretch only after strands are pulled taut which requires large local strains. Most of the stretched bonds are interfacial

bonds. Subsequently, these bonds break and the interfacial failure occurs.

An upper limit to the strain at which scission must occur is given in the minimal path lengths of the network. For a site on the bottom wall to which the network is bonded, there are many paths through the polymer network to the top wall. (One can equivalently start from the top and go to the bottom wall.) The shortest path defines the minimal path length P for that particular bottom wall bonding site. For a given system, there is a set of P, one for each bond of the network to the bottom wall. The simulations show that the average over all these P is related to the failure strain. Conversion of an individual value of P into a strain can be done via the relation, $\epsilon_P = (P - L_z)/L_z$. For $\epsilon > \epsilon_P$, some bond within the given minimal path must break. Using Dijkstra's method,[15] P has been calculated for all bonding sites on the bottom wall. The average minimal path $\langle P \rangle$ over all such bonding sites to the bottom wall is typically about 2 L_z. In the absence of another constraint, this implies the system can be strained almost 100% before significant scission. For system R1 the path with the smallest P has $\epsilon_P = 0.84$, and average P has $\epsilon_{\langle P \rangle} = 1.1$. These values are consistent with the span of scission events and ϵ_f for R1 given above. The average value $\epsilon_{\langle P \rangle}$ is within 10% of ϵ_f. This is consistent over the many different simulations that have been performed. Thus, scission is determined by a global and not a local constraint. In addition, shear simulations yield the same result.

The failure strain is still close to $\epsilon_{\langle P \rangle}$ when the cross-linkers are allowed to fully bond to the surface. Given a system such as R1 with only a single bond per cross-linker to the surface, it is clear that adding more bonds to the surface does not change the minimal paths. Dynamically forming the networks as outlined above and allowing multiple surface bonds yields a different network, R3. Because of the solid surface geometry and the constraints of bond length, at most three bonds can occur per cross-linker and a solid surface. While the network R3 is not identical to R1 due to the dynamical network formation, the distribution of minimal paths does not change significantly. The deformation sequence described above does not change except for one aspect. Failure in R3 is no longer interfacial, but cohesive. Thus, for both adhesive and cohesive failure, the failure strain is about equal to the strain corresponding to the average minimal path $\epsilon_{\langle P \rangle}$.

To provide a simpler model for theoretical treatment to further test the connectivity constraints, an ordered network is constructed. The ordered network is designed to minimize the constraints of connectivity resulting in large minimal paths. As in R1, the ordered network is 6-fold coordinated with two monomers between each cross-linker. The network is constructed using the body-centered cubic (bcc) lattice as a template (see Figure 2a). Cross-linkers are the central particles in the bcc cells yielding a 6-fold lattice. The z direction is the (111) lattice direction. There are two [111] planes each with three sites in the bcc cell. These sites represent strands which form a zigzag path between cross-linkers. This path is adjusted to achieve the correct density. The positions at the origin and at (1,1,1) in the bcc cell are vacant. Figure 2 shows the basic building block of the network and gives more details of the network geometry. The system is also created at $\rho = 0.8$ and then equilibrated to $T = 0.3$ and zero load. This system is

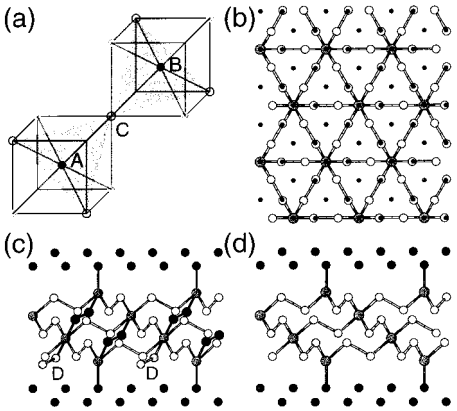

Figure 2. (a) Cross-linkers (A and B) are at the bcc lattice cell centers. Between the cross-linker planes are the strand planes (shaded region). A is below this strand plane and B is above. These two cross-linkers are bonded together through a strand at C. (b and d) Projections of O1 and O3 with cross-linkers (gray), walls (black), and strand beads (circles). The cross-linkers form layers of triangular lattices with an ABC stacking sequence. Part d shows the zigzag path between cross-linkers. Successive layers of cross-linkers are bonded together. (c) Dark circles represent the strands in O2 that connect next nearest cross-linkers. The dangling ends are labeled D.

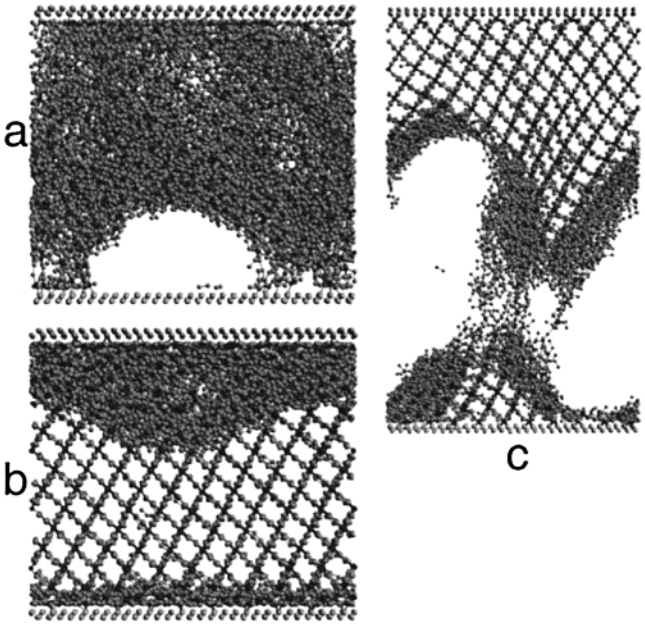

Figure 3. Images of systems under tensile strain show (a) the random, dynamically formed network R1 during failure, (b) the ordered network O1 at the same strain as part a, and (c) the ordered network O3 during failure. Image by Raster3d.[16]

labeled O1 as it also only has one bond per cross-linker to the surface.

In system O1, there are few constraints on the strands. When a tensile pull is applied to the ordered network, the strands can straighten out uniformly like an accordian. *All* strands are expected to become taut before any bond breaking occurs. Thus, this system should expand considerably more before failure than the random structures. In fact, even though the strands are very short and the temperature is below the glass transition temperature, this system should behave like an elastomer.

The stress−strain curve is shown in Figure 1 for the ordered system O1. The yield stress depending only on the LJ interactions is identical to the random network's.

As expected, failure occurs at a much larger strain, $\epsilon_f = 2.5$. The minimal paths are fully taut zigzag paths (see Figure 3b); all the minimal paths are identical. The strain for these taut paths at which the bonds must begin to stretch is $\epsilon_P = 2.3$ calculated directly from the geometry. The stress begins to rise sharply at this strain because the bonds are being stretched. Figure 3 shows that the strands open up as expected. The network does not open up uniformly; instead, it progressively opens up around an initial nucleation site determined by the combination of local disorder ($T < T_g$) and thermal fluctuations. The initial region grows with increasing strain spanning the system in the x direction. Then, layer by layer the rest of the strands straighten out. The noticeable rises in the stress−strain curve before the final rise are due to the extra stress it takes to pull the two layers at the walls which are more strongly packed. More force is need to pull the layers apart. Only after all the strands are taut, do the bonds begin to stretch and then break at the interface.

System O1 has a much larger failure stress than R1, even though the number of bonds to the solid surface are identical in the two systems. Because the O1 network completely opens before bond breaking occurs, more bonds break simultaneously. The ideal fracture stress for all interfacial bonds simultaneously breaking is

$$\sigma_{id} = F_{br} * N_b/A \tag{2}$$

where F_{br} is the force to break a bond, N_b is the number of bonds to the wall, and A is the wall area. O1 and R1 have $N_b = 60$ and $\sigma_{id} = 6.5$. The fracture stress of O1, $\sigma_f = 4.9$ is much closer to the ideal value than R1's value (3.4). For R1, interfacial bond breaking occurs over a strain range of 0.18, but for O1, the range is just 0.005. Thus, at any given strain fewer bonds are broken in R1, and the contribution to the stress by the bond forces is significantly smaller than for O1.

The reason for interfacial failure is perfectly clear for O1. The number of bonds at the interface is fewer than the number of bonds elsewhere in the network. The bond density $b(z)$ is calculated by counting the number of bonds per area that cross a z-plane at z. Near failure, the average bulk $b(z)$ is 0.55 for R1 and 0.26 for O1. Since R1 is near failure at a much lower strain, the density and thus the bond density is larger than for O1. In both cases $b(z)$ is just 0.09 at the interface. Thus, the stress is applied to fewer bonds at the interface. These bonds must stretch more to individually apply a larger force; consequently, they break first and failure occurs at the interface.

It is instructive to create an ordered network that fails cohesively. Constructing an ordered network with three bonds per cross-linker to the wall (O3) can easily be done. By positioning interfacial cross-linkers above the middle of the triangles of the wall fcc layer, the cross-links can bond to each particle in the triangle. In this case, the same number of bonds occurs for all cross-linkers. There should be no preference to failure at the interface. Given that the interface is a small fraction of the system, failure is likely to occur within the network—cohesively. The O3 system should completely open up under a tensile pull, just like system O1. Only the failure mode will be different. Thus, the failure strain in system O3 is expected be almost identical to O1; only slight differences due to more interfacial bonds being strained in O3 should occur.

Figure 3 shows that indeed cohesive failure occurs, and that the failure strain is slightly larger than for system O1. The stress−strain curve for O3 (Figure 1) matches that of O1 until the strain is close to the failure strain. The O3 failure stress is larger ($\sigma_f = 8.7$), since there are more bonds to break. However, σ_f is larger by only a factor of about 2, not three like the ideal value, $\sigma_{id} = 19.5$. All the bonds break at the interface in O1 in about 1000 time steps. For O3, 6000 time steps of bond breaking occur. As noted above, this results in a smaller σ_f for O1.

Systems O1 and O3 are on the extreme with respect to lack of constraints which allow for maximal failure strains. A more rigorous test of the minimal path concept would be a system designed to fail at a strain less than the failure strain for the random network R1. Such a system has been constructed. Large strains occur in O1 because of the lack of constraints between strands connecting cross-linkers in neighboring planes. A network with some strands connecting next nearest neighbor planes of cross-linkers should have fundamentally different behavior. Figure 2c shows the basic construction of such a system, O2. One of the three strands extending downward from every cross-linker is switched to connect to a next nearest cross-linker. This cannot be done for the cross-linkers two layers from the wall, resulting in some dangling ends. One could bond these ends to the walls, but here the wall bonding is kept the same as in O1. The random network R1 happens to have about the same number of dangling ends. The O2 stress−strain curve (Figure 1) exhibits failure at a *lower* strain and stress than R1. This lower failure strain agrees with the calculated minimal path strain $\epsilon_{\langle P \rangle} = 0.6$ directly determined from the taut path of connected next nearest neighbor cross-linkers.

IV. Discussion

Direct comparison with experimental measurements is not presently possible. The simulations discussed here have a thickness of about 20 nm which is much smaller than typically treated experimentally. Larger thicknesses, up to 60 nm, have been simulated.[9] In comparison to macroscopic systems, the simulations correspond to the small region near the surface. The connection between the simulations strain and stress and the macroscopic strain and stress is nontrivial. In tensile pull experiments the volume does not necessarily increase as it does in the simulations. However, this difference is not important, since simulations in (volume conserving) shear mode have been performed and the same results occur.

There are at least two intermediate factors which are important. Taking typical values for unfilled epoxies, the size of the plastic deformation zone is to be about 10 μm.[4] Thus, the simulation stress and strain correspond to that within the plastic zone which is poorly characterized experimentally. Another important factor is the homogeneity of the simulation systems. Once the strain field need not be homogeneous, segments of the minimal paths can become taut without the whole path being taut. In this way, significant bond breaking and consequently failure can occur at lower failure strains than $\epsilon_{\langle P \rangle}$. This effect has been seen in simulations performed with controlled defects that vary the number of interfacial bonds.[9] In particular, the failure strain decreases with increasing defect size. The mechanism by which the failure strain decreases involves interfacial

Table 1. System Size Dependence

no.	no. particles	L_z	$\epsilon_{\langle P \rangle}$	ϵ_f
1	51 500	19.9	0.97	1.05
2	91 000	39.2	0.92	1.02
3	170 000	77.6	0.93	1.00

segments of the minimal path being stretched taut before the whole path.

To be able to compare these simulation results with experiment requires that either the simulations must be performed on (much) larger systems or the experiments must be performed on nanometer thick systems. The result that the minimal paths determine failure strains is an important part of how to think about adhesive failure particularly at the molecular scale. This result must be combined with an understanding of other important aspects of adhesives such as defects, larger scale deformations, etc.

The correspondence of the minimal path lengths with the failure strain has been verified in several other of my simulations. System size is an important an issue to address. Table 1 gives the values of ϵ_f and $\epsilon_{\langle P \rangle}$ for larger random networks. These systems have a base area three times that of R1; consequently, there are about three times the number of minimal paths connecting the bonding sites on the walls yielding better statistics. The table data shows that $\epsilon_{\langle P \rangle}$ changes slightly with system size, but such that it matches the changes in ϵ_f. For the largest two systems, the system size effects appear to have saturated. This is consistent with the fact that the network structure is split between an interfacial region and "bulk" intermediate region. The interfacial region extends on a few bead diameters from the walls. Thus, at a wall separation much larger than a few bead diameters, the system structure will be dominated by the intermediate bulk structure and will not be dependent on the system size.

V. Conclusions

By manipulating only the network connectivity to vary the minimal paths connecting the two solid surfaces, the equality of the failure strain with the average minimal path has been demonstrated. Easy manipulation of the network connectivity is obtained by constructing simple, ordered networks. Using these ordered networks, the failure strain has been made smaller and larger than for dynamically cross-linked, random networks by directly changing the minimal paths.

Acknowledgment. This work was supported by the DOE under Contract DE-AC04-94AL8500. Sandia is a multiprogram laboratory operated by Sandia Corp., a Lockheed Martin Company, for the DOE.

References and Notes

(1) Zhou, S.; Beazley, D.; Lomdahl, P.; Holian, B. *Phys. Rev. Lett.* **1997**, *78*, 479.
(2) Cleri, F.; Yip, S.; Wolf, D.; Phillpot, S. *Phys. Rev. Lett.* **1997**, *79*, 1309.
(3) Baljon, A.; Robbins, M. *Science* **1996**, *271*, 482.
(4) Kinloch, A.; Young, R. *Fracture Behavior of Polymers*; Applied Science Publishers: London, 1983.
(5) Glad, M.; Kramer, E. *J. Mater. Sci.* **1991**, *26*, 2273.
(6) Wool, R. *Polymer Interfaces: Structure and Strength*; Hanser: Munich, Germany, 1995.
(7) Binder, K., Ed. *Monte Carlo and Molecular Dynamics Simulations in Polymer Science*; Oxford: New York, 1995.
(8) Kremer, K.; Grest, G. In *Monte Carlo and Molecular Dynamics Simulations in Polymer Science*; Binder, K., Ed.; Oxford: New York; 1995, Chapter 4, pp 194−271.
(9) Stevens, M. *Macromolecules* **2000**, *34*, 0000.
(10) de Gennes, P. *Scaling Concepts in Polymer Physics*; Cornell University: Ithaca, NY, 1979.
(11) Termonia, Y.; Meakin, P.; Smith, P. *Macromolecules* **1985**, *18*, 2246.
(12) Thompson, P. A.; Robbins, M. O. *Phys. Rev. A* **1990**, *41*, 6830.
(13) Schneider, J.; Hess, W.; Klein, R. *J. Phys. A* **1985**, *18*, 1221.
(14) Morgan, R.; Kong, F.-M.; Walkup, C. M. *Polymer* **1984**, *25*, 375.
(15) Hu, T. *Combinatorial Algorithms*; Addison-Wesley: Reading, MA, 1982.
(16) Merritt, E. A.; Bacon, D. J. *Methods Enzymol.* **1997**, *277*, 505.

MA0009505